Fish and Shellfish Immunology 166 (2025) 110596

Contents lists available at ScienceDirect

Fish and Shellfish Immunology

journal homepage: www.elsevier.com/locate/fsi

Full length article

Characterization of CD8$^+$ T Cells in large yellow croaker *Larimichthys crocea* and their dynamics in response to *Cryptocaryon irritans* infection

Guolong lai [a], Xinran Li [a], Sichang Liu [a], Luyang Zhao [a], Mengtian Xie [a], Li Huang [a], Wenxuan Zhang [a], Wenbing Bao [a], Yan Lin [a], Xinhua Chen [a,b,*], Yang Ding [c,**]

[a] State Key Laboratory of Mariculture Breeding, Key Laboratory of Marine Biotechnology of Fujian Province, College of Marine Sciences, Fujian Agriculture and Forestry University, Fuzhou, 350002, China
[b] Southern Marine Science and Engineering Guangdong Laboratory (Zhuhai), Zhuhai, 519000, China
[c] Department of Pathobiology, School of Veterinary Medicine, University of Pennsylvania, Philadelphia, PA, 19104, USA

ARTICLE INFO

Keywords:
Large yellow croaker *Larimichthys crocea*
Monoclonal antibody
CD8$^+$ T cells
Cryptocaryon irritans infection
Proliferation and depletion

ABSTRACT

CD8$^+$ T cells are critical cytotoxic effectors involved in pathogen clearance, including defense against parasitic infections in aquaculture species. In this study, we developed a monoclonal antibody specifically targeting the CD8α chain, enabling the identification of CD8$^+$ T cells in large yellow croaker *Larimichthys crocea* and providing a valuable tool for studying cytotoxic T cell responses in teleosts. Croaker CD8$^+$ T cells were more abundant in mucosal than systemic lymphoid organs, suggesting their preferential localization to sites of pathogen entry. Using this tool, we investigated CD8$^+$ T cell responses to *Cryptocaryon irritans* infection. During acute infection, CD8$^+$ T cells significantly proliferated in the spleen, head kidney (HK), and gills, accompanied by upregulation of cytotoxic genes including *granzyme a*, *granzyme b*, and *perforin 1*. Notably, a previously unrecognized depletion of CD8$^+$ T cells was observed in the spleen and HK, despite the total numbers of lymphocytes remaining unchanged. Our findings demonstrate an indispensable role of CD8$^+$ T cells as cytotoxic effectors involved in the defense against parasitic infection, and suggest their potential as valuable immunological biomarkers for disease monitoring or as targets for vaccine-based interventions in aquaculture.

1. Introduction

The adaptive immune system integrates humoral and cell-mediated immunity to provide vertebrates with a formidable defense against a broad spectrum of pathogens [1]. As key effectors of cell-mediated immunosurveillance, CD8$^+$ T cells, commonly known as cytotoxic T lymphocytes (CTLs), play an indispensable role in adaptive immunity by exerting cytotoxic activity to eliminate viral infections, intracellular bacteria, and tumor cells in mammals [2]. CD8$^+$ T cells are characterized by the surface expression of CD8α and CD8β co-receptor chains, which form the CD8 heterodimer encoded by two adjacent genes within the *cd8* locus. This heterodimer defines the predominant CD8$^+$ T cell subset, commonly referred to as CD8αβ T cells [3,4]. During T cell priming, the CD8αβ heterodimer binds to major histocompatibility complex class I (MHC I) molecules on antigen-presenting cells (APCs), thereby enhancing the sensitivity and specificity of antigen recognition [5]. In rare cases, a small population of CD8$^+$ T cells expressing CD8αα but lacking surface CD8β has been found to reduce the antigen sensitivity of the T cell receptor (TCR), a feature considered inconsistent with its typical co-receptor function [6].

Over the past decades, our understanding of teleost CD8$^+$ T cells has remained largely at the molecular and transcriptional levels, primarily due to the lack of effective immunological tools. Even so, these foundational studies have laid the groundwork for our current knowledge of *cd8* gene distribution and expression dynamics. For instance, *cd8* genes have been identified in several fish species, including rainbow trout (*Oncorhynchus mykiss)* [7], fugu (*Takifugu rubripes*) [8], ginbuna crucian carp (*Carassius auratus*) [9], mandarin fish (*Siniperca chuatsi*) [10], Japanese flounder (*Paralichthys olivaceus*) [11], and these genes have been shown to be transcriptionally upregulated in response to agonist stimulation or infections with viral, bacterial, and parasitic pathogens [7–11]. It is worth noting that a clear correlation has been observed

* Corresponding author. State Key Laboratory of Mariculture Breeding, Key Laboratory of Marine Biotechnology of Fujian Province, College of Marine Sciences, Fujian Agriculture and Forestry University, Fuzhou, 350002, China.
** Corresponding author.
E-mail addresses: chenxinhua@tio.org.cn (X. Chen), dinyang@vet.upenn.edu (Y. Ding).

https://doi.org/10.1016/j.fsi.2025.110596
Received 30 May 2025; Received in revised form 3 July 2025; Accepted 24 July 2025
Available online 24 July 2025

between cell-mediated cytotoxicity and the expression of *cd8α* and/or *cd8β* genes in surface IgM$^-$ leukocytes, supporting the presence of cytotoxic CD8$^+$ T cells in teleost species [12]. With technological advances, the advent of refined research tools, particularly the development of monoclonal and polyclonal antibodies (mAbs and pAbs), has enabled the isolation and identification of CD8$^+$ T cells in several fish species, thereby confirming the previously observed correlations were more than mere coincidence [13–16].

The use of specific anti-CD8 mAb has provided an exceptional opportunity to advance our understanding of the dynamics, abundance, and functional roles of CD8$^+$ T cells in fish species, particularly in response to aquatic pathogens in both direct and indirect settings. In teleosts, CD8$^+$ T cells are primarily distributed in systemic lymphoid organs, including the thymus, head kidney, and spleen [16,17]. Yet it is worth noting that CD8$^+$ T cells have also been found to accumulate within the intraepithelial regions of various mucosa-associated lymphoid tissues (MALTs), such as the intestines, gills and skin, highlighting their important role in immunosurveillance at mucosal barriers directly exposed to environmental pathogens [18–20]. Moreover, recent studies pointed out that fish CD8$^+$ T cells are involved in antiviral defense during the early stages of infection [21] and that they can execute innate cell-mediated cytotoxicity to eliminate parasites in a contact-dependent manner [22]. Notably, this cytotoxic activity can be further enhanced through immunization with parasite-derived heat shock protein 70C as demonstrated in *Cryptocaryon irritans* (Ci) -infected orange spotted grouper (*Epinephelus coioides*) [23]. Taken together, these findings underscore the role of fish CD8$^+$ T cells in providing both systemic and local protective immunity to the host, functionally convergent with their mammalian counterparts.

In the present study, we developed a monoclonal antibody (mAb) specific to CD8α from large yellow croaker *Larimichthys crocea*, which enabled us to isolate and identify CD8$^+$ T cells in this species. Using this newly established tool, we further characterized the tissue distribution and proliferative dynamics of CD8$^+$ T cells during infection with the common marine parasite Ci [24], which causes cryptocaryoniasis outbreaks that have posed a significant threat to marine aquaculture. Cryptocaryoniasis leads to high mortality rates, stunted growth, and other secondary pathological effects in infected fish. However, traditional treatment methods such as chemotherapeutics are often ineffective or impractical in open aquaculture systems [25]. The resulting reduction in market value, particularly in species like pompano and large yellow croaker, contributes to more than $100 million in economic losses annually, posing ongoing challenges to the sustainability and productivity of the marine aquaculture industry [25,26]. Notably, during the early stages of Ci infection, an acute depletion of CD8$^+$ T cells was observed in systemic immune tissues, which could not be compensated by proliferative responses under lethal infection stress. In contrast, this uncompensated depletion was not evident in the gills, which serve as the primary site of infection, highlighting that the rapid and extensive loss of CD8$^+$ T cells may represent a critical factor contributing to the high mortality of fish suffering from widespread Ci outbreaks in aquaculture.

2. Material and methods

2.1. Animals and ethics statement

Large yellow croakers with 100.0 ± 5.0 g in weight were purchased from a mariculture farm in Ningde, Fujian, China and acclimated in our fish facility for at least 2 weeks. Fish were raised at 20 °C in an aerated recirculating seawater system equipped with internal biofilters and UV sanitation system manufactured by Shanghai Haisheng Biotech Co., Ltd, and fed daily with commercial pellet diets at 1 % biomass/day. Regarding the Ci infection experiment, fish were randomized to the control and infection groups and kept in individual flow-through seawater tanks, respectively. All animal experiment procedures were approved by the Laboratory Animals Ethics and Welfare Committee of Fujian Agriculture and Forestry University according to the Laboratory animal Guideline for ethical review of animal welfare (GB/T 35,892–2018) and performed in compliance with the Regulations of the Administration of Affairs Concerning Experimental Animals established by the Fujian Provincial Department of Science and Technology. All efforts were made to minimize the pain of animals.

2.2. Cell culture

Human embryonic kidney 293T (HEK293T) were purchased from the China Center for Type Culture Collection (CTCCC). The mouse myeloma SP2/0 and embryonic fibroblasts NIH/3T3 was purchased from the Shanghai Zhongqiaoxinzhou Biotech. HEK293T, SP2/0 and NIH/3T3 cells were cultured in Dulbecco's Modified Eagle Medium (DMEM, Gibco) supplemented with 10 % Fetal Bovine Serum (FBS, Gibco) and 1 % penicillin/streptomycin solution (Gibco). All cell lines were maintained at 37 °C in 5 % CO_2 in a water-saturated cell incubator.

2.3. Sequence analysis

The cDNA and amino acid sequence of CD8α of large yellow croaker (referred as croaker CD8α throughout the paper) were obtained from the whole-genome sequence with the accession number JRPU02000000 and the project PRINA245366 in National Center for Biotechnology Information (NCBI) GenBank (https://www.ncbi.nlm.nih.gov/nuccore/IRPU00000000.2/) [27]. The locations and gene structure information were retrieved from Genome Data Viewer in the NCBI. The tertiary structures of indicated proteins were predicted by SWISS-MODEL and were visualized by PyMOL. Protein functional domains were predicted using SMART. Multiple sequence alignment was performed using DNAMAN and was displayed with homology analysis. Phylogenetic tree was built in MEGA11 using neighbor-joining (NJ) method with 500 bootstrap replications. Accession numbers for these sequences used were listed in Supplementary Table 1.

2.4. Preparation of NIH/3T3 cells expressing croaker CD8α protein

To produce the recombinant protein of croaker CD8α, the sequence encoding the extracellular and transmembrane domain containing signal peptide of croaker *cd8α* was cloned into pCDH-CMV-EF1-GFP-Puro plasmid (System Biosciences) as previously described [28] that expresses a GFP protein as indicator. Subsequently, resulting plasmid (referred as pCDH-CD8α/GFP) and two helper plasmids including psPAX2 and pMD2.G (Addgene) were co-transfected into HEK293T cells by using Lipo8000™ Transfection Reagent (Beyotime) to package the retrovirus expressing croaker CD8α/GFP fusion protein. NIH/3T3 cells were then infected with the recombinant retrovirus in the presence of polybrene (Beyotime) following the manufacturer's instructions. The resulting NIH/3T3 cells stably express croaker CD8α/GFP fusion protein (NIH/3T3-CD8α/GFP) were next selected with 5 μg/ml puromycin (Beyotime). The expression of CD8α/GFP fusion protein on NIH/3T3 cells was verified by confocal fluorescence microscope (Leica STELLARIS 5) indicated by GFP fluorescence and the purity of the GFP expressing was confirmed by flow cytometry (BD Accuri C6 Plus) before the immunization.

2.5. Development of monoclonal antibodies (mAbs) against croaker CD8α

BALB/c mice were immunized with ten million NIH/3T3 cells firmly expressing croaker CD8α in PBS by intraperitoneal (*i.p.*) injection weekly for four times, following the standard protocol established by animal facility of Fujian Agriculture and Forestry University. Three days after the last immunization, BALB/c mice were sacrificed and splenocytes were harvested and fused with SP2/0 cells in the presence of

polyethylene glycol following the manufacturer's instructions (Sigma). The resulting fused cells were seeded in the medium containing Hybridoma Feeder (Biodragon) with concentration hypoxanthine, aminopterin and thymidine [4] (Biodragon) for selection and cultured over 7 days. The hybridoma (clone 5E3) consistently secreting mAbs against croaker CD8α was selected and the isotype of mAbs were determined with the Mice Ig Isotyping ELISA Kit (Biodragon). The specificity of anti-croaker CD8α was validated by only staining croaker CD8α/GFP expressing NIH/3T3 cells but not GFP expressing cells. The chosen hybridoma clone was then *i.p.* injected into nude mice to generate ascites following the standard protocol established by animal facility of Fujian Agriculture and Forestry University. The anti-croaker CD8α mAb were purified from the ascites using a HiTrap protein G column (GE Healthcare) according to the manufacturer's instructions.

To validate the specificity of the developed anti-croaker CD8α monoclonal antibody, the extracellular domain of *cd8* was subcloned into the pCMV-Myc vector (Takara) and expressed in HEK293T cells as described above. Forty-eight hours after transfection, cells were collected and lysed in RIPA buffer at a concentration of 1×10^7 cells/ml (Beyotime). A total of 30 μl of the cell lysate was separated by 4 %–20 % SDS-PAGE and transferred onto a polyvinylidene difluoride (PVDF) membrane (Bio-Rad, USA). Western blotting was performed as previously described [29]. Briefly, the membranes were blocked with 5 % skim milk (BioRad) in PBS and incubated with either mouse anti-croaker CD8α mAb (1 μg/ml) or mouse anti-myc (1 μg/ml, Proteintech). The membranes were then detected with HRP-conjugated anti-mouse IgG (0.2 μg/ml, GE Healthcare). Immunoreactive bands were visualized using Immobilon Western Chemiluminescent HRP Substrate (Millipore, USA) and analyzed with Azure Biosystems C500.

2.6. Ci infection

Ci were isolated and used to infect large yellow croaker as previously reported [30]. Briefly, Ci-infected croakers identified by intensive white spots on the gills and skin were quarantined in flow-through tanks to development trophont. Once the trophonts matured and detached from the host fish, protomonts were collected from the tank and then incubated at 26 °C for 24–48 h until the infectious theronts were released from tomonts. For acute parasite infection, fish were exposed to a single dose of ~8000 theronts per fish in an aerated flow-through tank with water flow shut down for 12 h to ensure sufficient Ci infection. Control fish were maintained in a separate Ci-free flow-through tank and subjected to the same procedure as Ci-infected fish. The survival rates of croakers following Ci infection were monitored to calculate mortality and to ensure the consistency and reproducibility of the infection model used for subsequent experiments.

To evaluate the proliferation of croaker CD8α$^+$ T cells upon Ci infection, large yellow croakers were anesthetized with MS-222 (50 mg/L) and *i.p.* injected with 250 μg of 5-ethynyl-2′-deoxyuridine (EdU, Invitrogen) dissolved in 100 μl PBS per fish 24 h before sampling. Large yellow croaker was euthanized at 3- and 7-days post Ci infection with an overdose of MS-222 (100 mg/L) according to the manufacturer's instructions, and head kidney, spleen and gills were extracted for the isolation of leukocytes.

2.7. Isolation of leukocytes

To assess the CD8α$^+$ T cells by flow cytometry, large yellow croaker was euthanized as described above, and leukocytes were isolated from head kidney, spleen, liver, gills, gut and periphery blood according to our previous report [31]. Briefly, the sacrificed fish were perfused with PBS-heparin (Sigma-Aldrich) through the heart to remove the circulating blood from the vessels associated to the MALTs. The tissues mentioned above were then removed and pushed through 70-μm cell strainers (BD) with ice-cooled DMEM medium (Gibco) supplemented with 2 % FBS (Gibco) and 1 % Penicillin-Streptomycin (Gibco). Periphery blood was drawn from the caudal vein and immediately diluted 10 times with the above supplemented DMEM/2 % FBS additionally containing 15 IU/ml heparin sodium (Sigma-Aldrich). The resulting cell suspensions were gently layered onto a 51 %/34 % discontinuous Percoll density-gradient (GE Healthcare) and centrifuged at 650 g for 30 min at 4 °C with the lowest acceleration and deceleration for the separation of leukocytes. The buffy coat, located between the 34 % and 51 % Percoll layers was collected and washed twice by DMEM/2 % FBS. Thereby, the isolated large yellow croaker leukocytes were resuspended with the same buffer and kept on ice until further use.

2.8. Flow cytometry and cell sorting

To identify croaker CD8α$^+$ lymphocyte population, the leukocytes isolated from head kidney (HKL), spleen (SPL), liver (LVL), gills (GILs), gut (GTL), and blood (PBL), were stained with anti-croaker CD8α mAb (2 μg/ml, mouse IgG1 isotype), and then detected by goat anti-mouse IgG-FITC pAb (Abcam, 1 μg/ml). Incubations of primary and secondary Abs were performed in DMEM/1 % FBS on ice for 30 min and washed twice with DMEM/1 % FBS after each staining. Mouse IgG1 isotype (Biolegend; 2 μg/ml) was applied as isotype control for primary Ab staining. All the samples were analyzed by NovoCyte Advanteon flow cytometer, and data were analyzed using FlowJo. Regarding cell sorting, the stained SPL, HKL and GIL as mentioned above were applied to BD FACS Aria II flow cytometer to sort CD8α$^+$ lymphocytes for further gene expression analyses (BD Biosciences). The purity of the sorted CD8α$^+$ cell populations was assessed by analyzing an aliquot of each sample by flow cytometry, and the purity of all preparations used for gene expression analysis ranged from 96 % to 99 % (Supplementary Fig. 1). Additionally, the stained SPLs were examined under a microscope for the cytological analysis of CD8α$^+$ T cells.

To quantify and compare the differences in cell numbers between control and Ci-infected fish, we collected the entire spleen, HK and all eight gill arches from croaker. Leukocytes were isolated in parallel from each tissue, with all samples processed using identical volumes of cell culture medium and staining solutions to ensure consistency. This standardized approach ensured that the number of cells obtained reflected the total cellularity of each tissue, enabling accurate and comparable quantification across groups. During flow cytometry analysis, all samples were acquired at the same flow rate, and absolute cell numbers were calculated as the number of events per second. This method allowed us to directly assess Ci-induced changes in the total lymphocyte population and the abundance of CD8$^+$ subsets in immune-relevant tissues, while avoiding reliance on relative percentages that may be affected by shifts in other lymphocyte subsets.

2.9. Immunofluorescence microscopy

To elucidate the specificity of mouse anti-croaker CD8α mAb, we generated a control NIH/3T3 cell line that stably expressed GFP protein (tag protein on empty pCDH plasmid) as described above (NIH/3T3-GFP). The staining of NIH/3T3-CD8α/GFP or NIH/3T3- GFP cells for detection of CD8α were performed as mentioned in Flow cytometry and cell sorting section, except that the secondary pAb was replaced with goat anti-mouse IgG-APC (Abcam, 1 μg/ml). The stained NIH/3T3 cells and aforementioned SPLs were then fixed and permeabilized with Fixation/Permeabilization Solution (BD) for 20 min at room temperature. Cell nuclei were stained with DAPI (1 μg/ml; Sigma-Aldrich) and the slides were mounted with Fluoroshield (Abcam). Images were acquired by using a Leica DM6000 fluorescence microscope (STELLARIS 5) and analyzed with LAS X software.

2.10. Quantitative real-time PCR (qPCR)

Total RNA was extracted from sorted croaker CD8α$^+$ and CD8α$^-$ fractions by using RNAprep Pure Micro Kit (TIANGEN) and RNA reverse

transcription were performed by 2 × NovoScript Plus 1st Strand cDNA Synthesis SuperMix (Novoprotein) following the manufacturers' instructions. To confirm the expression of marker genes for T and B cells in the sorted cells, PCR reaction was performed with KeyPo SE Master Mix (Vazyme). The amplification was carried out with initial activation of the enzyme at 94 °C for 2 min, followed by 35 cycles of the following: 98 °C for 10 s, annealing at 55 °C for 30 s, and 68 °C for 30 s, and a final holding temperature of 4 °C. For quantification of gene expression in CD8α$^+$ T cells sorted from gills of Ci-infected and control fish, qPCR analysis was conducted with ChamQ Universal SYBR qPCR Master Mix (Vazyme) by a QuantStudio 5 Real-Time PCR Instrument (Thermo Fisher). Briefly, the reaction was conducted with initial activation of the enzyme at 95 °C for 30 s, followed by 40 cycles of the following: 95 °C for 10 s, annealing at 60 °C for 30 s, and a melt curve collection procedure. Primer sequences used are listed in Supplementary Table 2.

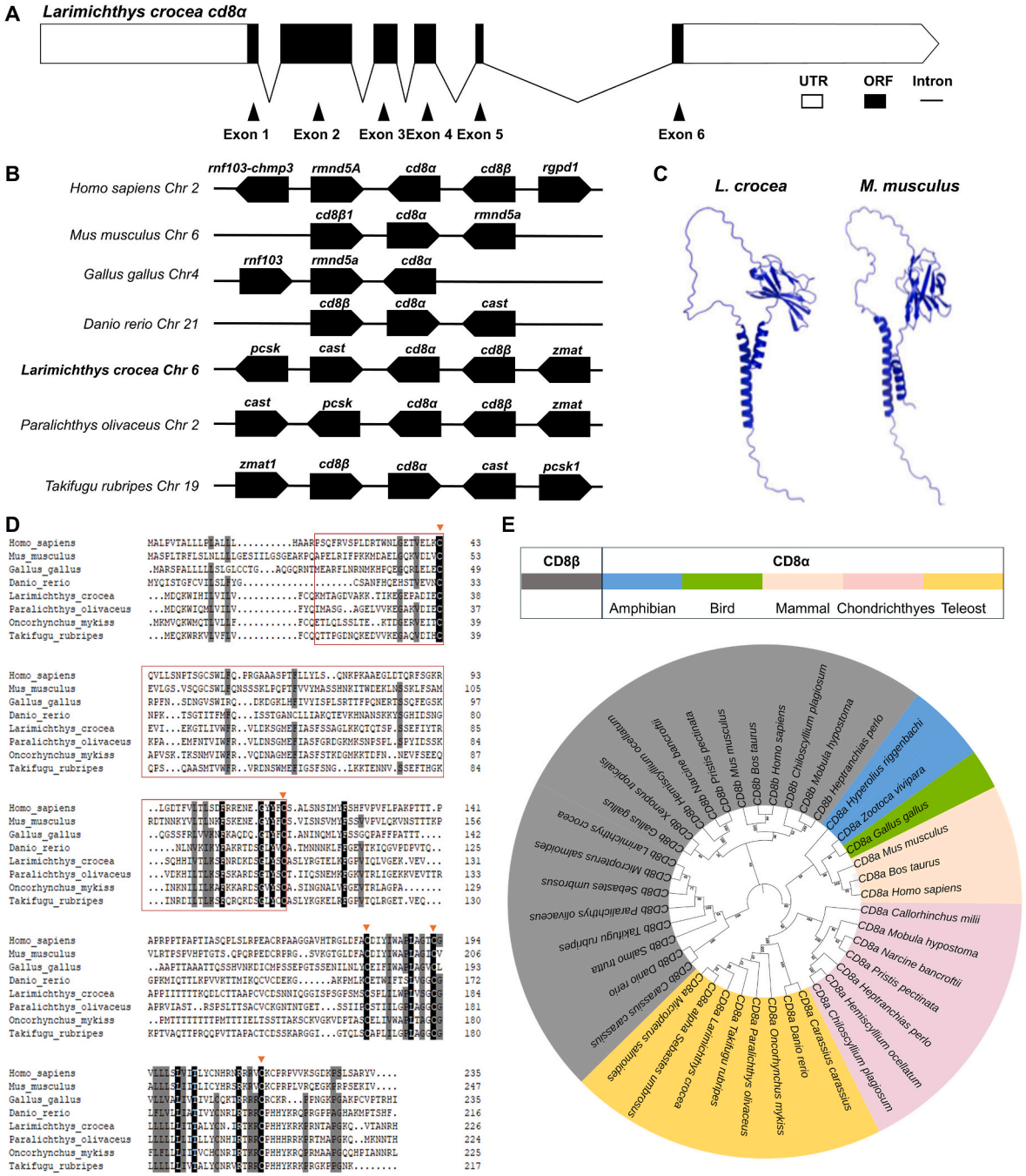

Fig. 1. Sequence and phylogeny analysis of croaker CD8α.
(A) Genomic structure of large yellow croaker *cd8α*. (B) Schematic representation of gene synteny at the *cd8α* loci in large yellow croaker and other species. The arrows indicated the transcriptional direction. The comparison does not reflect the virtual gene distance. (C) The tertiary structures of large yellow croaker and mouse CD8α predicted by SWISS model. (D) Multiple sequence alignments of large yellow croaker CD8α. Amino acid residues with 100 % identity are shown in black. The conserved cysteine residues which may be involved in the formation of intramolecular disulfide bonds are indicated by orange arrows. The typical conserved IG-like domain is boxed with red frame line. (E) Phylogenetic tree of CD8α and CD8β subunits built on the genetic distances of deduced amino acid sequences. The GenBank accession numbers for obtaining CD8α and CD8β amino acids sequences are provided next to the respective species names. (For interpretation of the references to colour in this figure legend, the reader is referred to the Web version of this article.)

2.11. Statistical analyses

All the sample sizes (n) and number of independent experiments are summarized in Supplementary Table 3 and indicated in the figure captions. Fish were always sampled in a randomized way, and all experiments were at least duplicated. Two-tailed Unpaired Student's *t*-test, and ordinary one-way ANOVA followed by Tukey's post hoc test were performed in GraphPad Prism (version 10). Normal distribution was checked using Levene's test. Significant differences were considered when P value < 0.05.

3. Results

3.1. Analysis of large yellow croaker cd8α gene and protein sequences

The predicted croaker *cd8α* gene (Gene ID: 104928930) was obtained from Genome assembly L_crocea_2.0 by accession number GCA_000972845.2 through NCBI GenBank database. Croaker *cd8α* gene sequence was cloned from head kidney (HK) cDNA and confirmed that the open reading frame is 687 base pair (bp), encoding a 228-amino acids protein, where a 15-aa signal peptide was predicted at N-terminus and an Immunoglobulin (Ig)-like domain located between Glu16-Cys107 (Supplementary Fig. 2). The determined genomic *cd8α* sequence is 3252 bp in length and is located on the Chromosome 6, comprising 5 introns and 6 exons (Fig. 1A). Gene synteny analysis revealed that croaker *cd8α* is adjacent to *cd8β*, a conserved arrangement between mammals and teleost fish. Additionally, a gene cluster containing *pcsk1-cast- cd8α-cd8β-zmat1* was found conserved in 3 out of 4 analyzed fish (Fig. 1B). As predicted by SWISS model based on the mouse CD8α structure, the tertiary structure of deduced croaker CD8α protein consists of three α-helices, ten β-sheets, and one disulfide bond formed by Cys38 and Cys107, resembling that of the mouse CD8α molecule. This structural conservation suggests a preserved functional framework that croaker CD8α is potentially crucial for its immune roles in interacting with MHC I and activating $CD8^+$ T cells (Fig. 1 C). Multiple sequence alignments showed that croaker CD8α protein shares 5 conserved cysteine residues, and 1 conserved Ig-like domain across different species (Fig. 1 D). Phylogenetic tree was constructed using both CD8α and CD8β subunits that confirmed croaker CD8α was clustered into the same clade formed by CD8 molecules from other teleost and higher vertebrates, while separated from another major branch made up of CD8β subunits from all analyzed species (Fig. 1E). Homology comparison revealed that croaker CD8α chain shares a relatively high identity (30.9–56.6 %) with CD8α from other teleosts, but exhibits lower

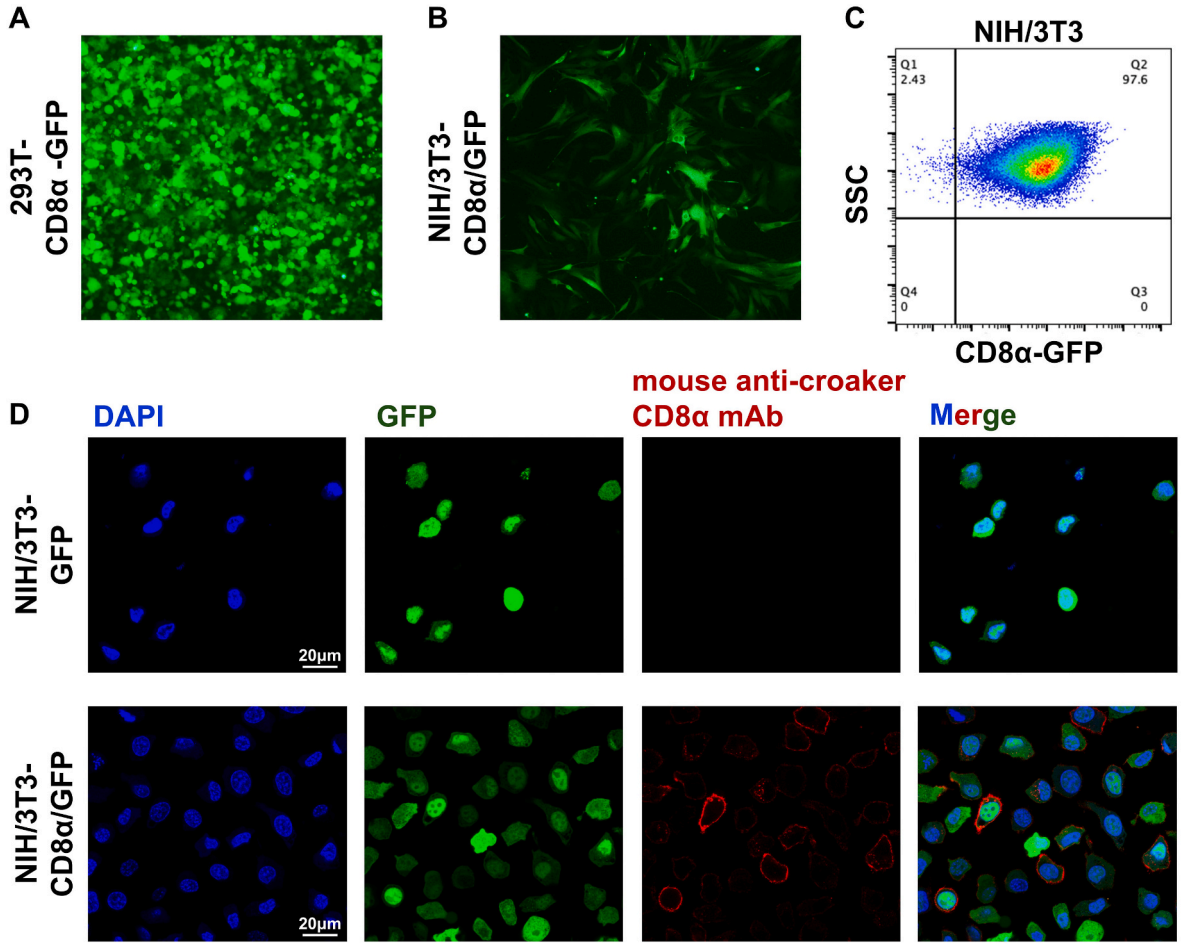

Fig. 2. Development of mouse anti-croaker CD8α mAb by immunization with CD8α expressing cells.
(A) Fluorescence microscopy of HEK293T cells that packaged recombinant retroviral vectors containing croaker CD8α fragment. (B, C) Fluorescence microscopic (B) and flow cytometry (C) analysis of NIH/3T3 infected by retrovirus expressing croaker CD8α/GFP fusion protein. NIH/3T3 cells expressing croaker CD8α were shown in green by microscopy in (A and B) NIH/3T3-CD8α/GFP cells were used to immunize mice once the purity of GFP-positive cells exceeded 97 % assessed by flow cytometry for the development of mAbs. (D) Specificity analysis of the newly developed mouse anti-croaker CD8α mAb. NIH/3T3-CD8α/GFP and NIH/3T3-GFP cells were incubated with mouse anti-croaker CD8α mAb and analyzed by fluorescence microscopy. Cells expressing GFP are green, cells co-stained with anti-CD8α are red on surface, nuclei are stained with DAPI (cyan). Scale bar = 20 μm. (For interpretation of the references to colour in this figure legend, the reader is referred to the Web version of this article.)

identity (19.9–26.5 %) with its homologues in tetrapods (Supplementary Table 4). Taken together, these analyses suggest that large yellow croaker CD8α molecule was highly conserved across species throughout evolution.

3.2. Development of mouse anti-large yellow croaker CD8α mAb

A conventional approach to produce antigen-specific Abs is to immunize mice using mouse derived NIH/3T3 cells that express certain antigen [32]. In this study, we used HEK293T cells to package a lentivirus expressing the croaker CD8α/GFP fusion protein (Fig. 2A), from which the packaged recombinant lentivirus was collected and subsequently applied to infect NIH/3T3 cells (Fig. 2B). The resulting CD8/GFP-expressing-NIH/3T3 cells were confirmed by flow cytometry to make sure more than 97 % were GFP-positive before immunization (Fig. 2C). Mice were sacrificed after four immunizations and anti-croaker CD8α mAb was produced and purified as previously described by us [33]. The selected anti-CD8α mAb clone 5E3 did not cross-react with the GFP-expressing-NIH/3T3 cell but specifically recognized the cell surface of CD8α/GFP-expressing-NIH/3T3 cells (Fig. 2D). Western blot analysis further confirmed that the anti-croaker CD8α mAb specifically recognized the CD8α protein expressed in transfected HEK293T cells (Supplementary Fig. 3) Collectively, both immunofluorescence and Western blot analyses verified the specificity of the produced anti-CD8α mAb against croaker CD8α antigens.

3.3. Identification of large yellow croaker CD8α$^+$ lymphocytes

Fish head kidney is a key lymphoid organ rich in T lymphocytes [34]. To identify CD8α-expressing leukocytes in large yellow croaker, the whole HK leukocytes were stained with the anti-CD8α mAb or isotype control Ab (mouse IgG1), then analyzed by flow cytometry and confocal immunofluorescence microscopy. Flow cytometry analysis revealed that the HKL expressing surface CD8α were exclusively located within the lymphocyte population, indicating that the CD8α-positive leukocytes are indeed lymphocytes (Fig. 3A and B). Whereas the isotype control Ab stained negligible cells under the same gating strategy (Fig. 3A–C). FACS (fluorescence-activated cell sorting)-sorted CD8α-positive lymphocytes from the HK, spleen and gills exclusively expressed the transcripts of *cd8α*, *cd8β* and the T cell marker gene *cd3ε*, while showing negligible expression of the CD4$^+$ T cells co-receptor genes, *cd4-1* and *cd4-2*, and two major B cell markers, *ighm* and *ight* which detect both surface and

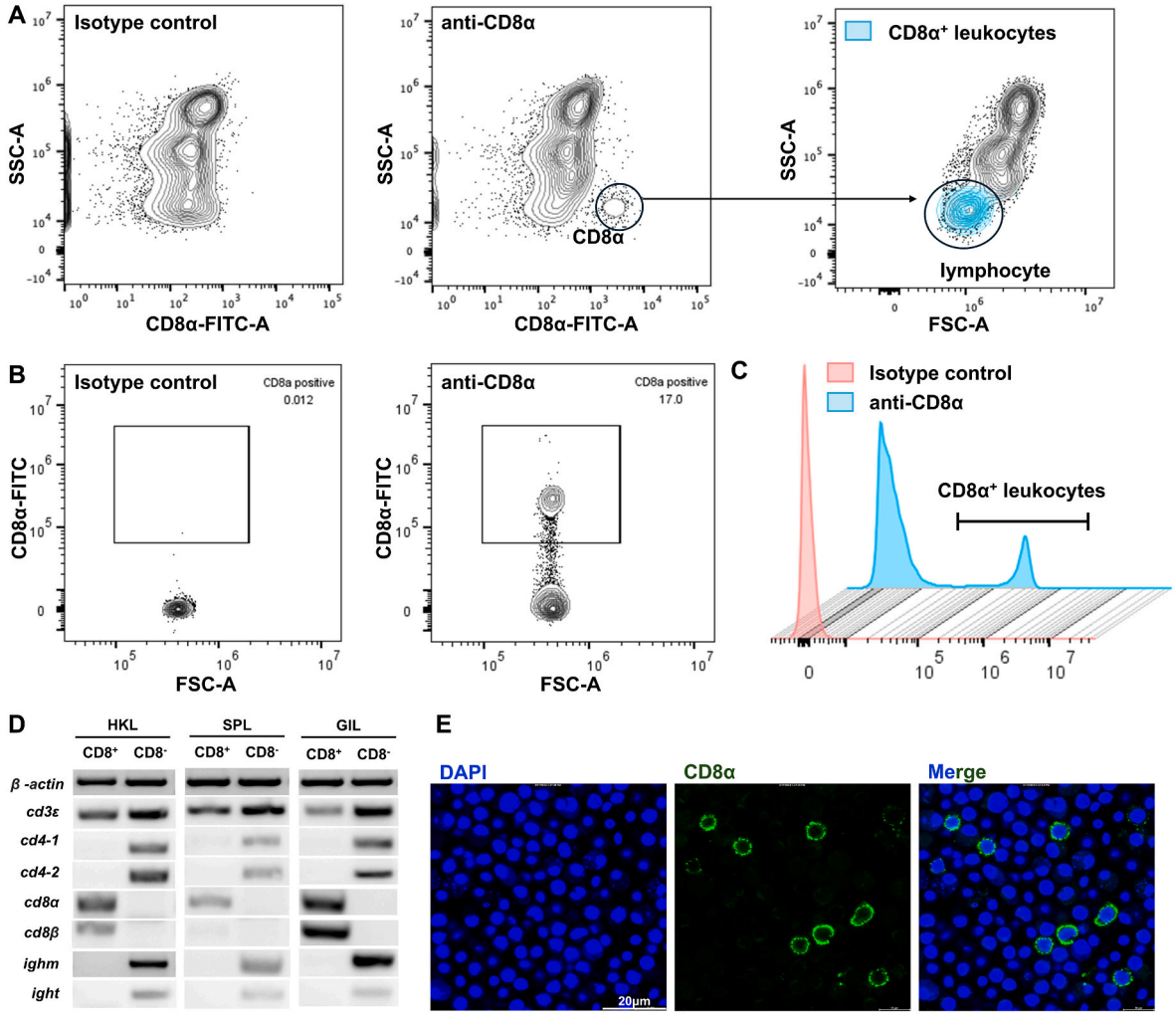

Fig. 3. Characterization of large yellow croaker HK leukocytes expressing surface CD8α.
(A) Flow cytometry analysis of croaker CD8α expressing HK leukocytes. Representative dot plots represent HKLs stained with mouse IgG1 isotype control Ab (left panel) or mouse anti-croaker CD8α mAb (middle panel). The CD8α$^+$ cells are circled from whole HKLs (middle panel) and appeared to be located within lymphocyte population as shown in blue (right panel). (B, C) Representative dot plot (B) and stagger offset histogram (C) show stained CD8α$^+$ T lymphocytes within the lymphocyte gate. (D) Gene expression profiles of CD8$^+$ and CD8$^-$ lymphocytes from the indicated tissues were measured by PCR. (E) Immunofluorescence showed spleen leucocytes that stained with anti-CD8α mAbs. Nuclei are counterstained with DAPI (blue). Scale bar = 20 μm. Data in A to E are representative of three independent experiments. (For interpretation of the references to colour in this figure legend, the reader is referred to the Web version of this article.)

secreted forms of IgM and IgT (Fig. 3D). In contrast, the expression of *cd8α* and *cd8β* in the CD8α-negative fraction was undetectable (Fig. 3D), confirming that our anti-croaker CD8α mAb specifically recognized all $CD8^+$ T cells expressing both CD8α and CD8β.

Under confocal immunofluorescence microscopy, croaker $CD8^+$ T cells exhibited typical lymphocyte morphology, appearing as round with a centrally located large, unsegmented nucleus and a thin, discontinuous rim of punctate staining on the cell surface (Fig. 3E).

3.4. Distribution of croaker $CD8^+$ T cells in lymphoid tissues

We next evaluated the abundance of croaker $CD8^+$ T cells in both systemic and mucosa-associated lymphoid tissues by flow cytometry. The results showed a substantial presence of $CD8^+$ T cells across all tissues examined (Fig. 4A and B). In case of systemic lymphoid tissues, a significant proportion of $CD8^+$ T cells was observed within the lymphocyte gates from HK (~14.1 %), spleen (~12.2 %), and liver (~15.8 %) (Fig. 4C). To our surprise, the frequency of $CD8^+$ T cells in gut was remarkably higher than in other tissues, making up an average of ~30.7 % of total lymphocytes, whereas the percentage in another mucosal tissue, the gills, was relatively moderate (~17.7 %) (Fig. 4C). It is noted that the abundance of $CD8^+$ T cells in PBL was considerably low, constituting only ~3.07 % of blood lymphocytes (Fig. 4C).

3.5. Proliferation of $CD8^+$ T cells in response to Ci infection

To further understand whether $CD8^+$ T cells are involved in the defense against pathogens, we infected croaker with Ci and assessed $CD8^+$ T cell proliferation using EdU in the spleen, head kidney, and gills. Ci is a well-known parasite that preferentially invades the gills in croaker [35]. Under the experimental conditions in our facility, Ci parasitizes the host for about 7–10 days before detachment. The infection dose of Ci theronts resulted in approximately 80 % cumulative mortality by 8 days post infection (Supplementary Fig. 4). After 3 days post infection (DPI), a significant increase in proliferation of $CD8^+$ T cells was observed only in the spleen, where the percentage of proliferating cells in infected fish (~19.3 %) was ~1.9-fold higher than that in control fish (~10.1 %) (Fig. 5A). By contrast, no changes of $CD8^+$ T cell proliferation were detected in the HK and gills between infected and control groups, suggesting that $CD8^+$ T cell proliferation in HK and gills had not yet been initiated in response to the infection at day 3 (Fig. 5B and C). However, at day 7 after infection, a large degree of $CD8^+$ T cell proliferation was evident not only in the spleen (Fig. 5D), but also in the HK (Fig. 5E) and gills (Fig. 5F), coinciding with the maturation of Ci and its imminent detachment from the host. The frequencies of dividing $CD8^+$ T cells in control fish were approximately 3.5 %, 5.9 %, and 2.6 % in the spleen, HK, and gills, respectively. In infected fish, these frequencies increased to 18.8 %, 21.4 %, and 12.9 % in the corresponding tissues, representing 5.4-fold, 3.6-fold, and 5.0-fold increases compared to control fish (Fig. 5D–F). These results demonstrate that $CD8^+$ T cells undergo a profound proliferation in response to Ci infection, especially at the late stage of infection while trophonts matured and detached, indicating their critical role in the immune defense against parasitic invasion.

3.6. Gene regulation in $CD8^+$ T cells sorted from gills upon Ci infection

$CD8^+$ T cells mediate their functions by secreting cytokines and cytotoxic granules to eliminate the infected cell or invading pathogens once recruited to the location of infection and tissue injuries [36]. To evaluate the effector capacity of croaker $CD8^+$ T cells at the site of infection, we sorted $CD8^+$ T cells from the gills lymphocytes 7 days after Ci infection and investigated the expression of genes associated with their activation and function. In these experiments, the transcript levels of marker gene *cd8α* and chemokine receptor *ccr7* in gills $CD8^+$ T cells

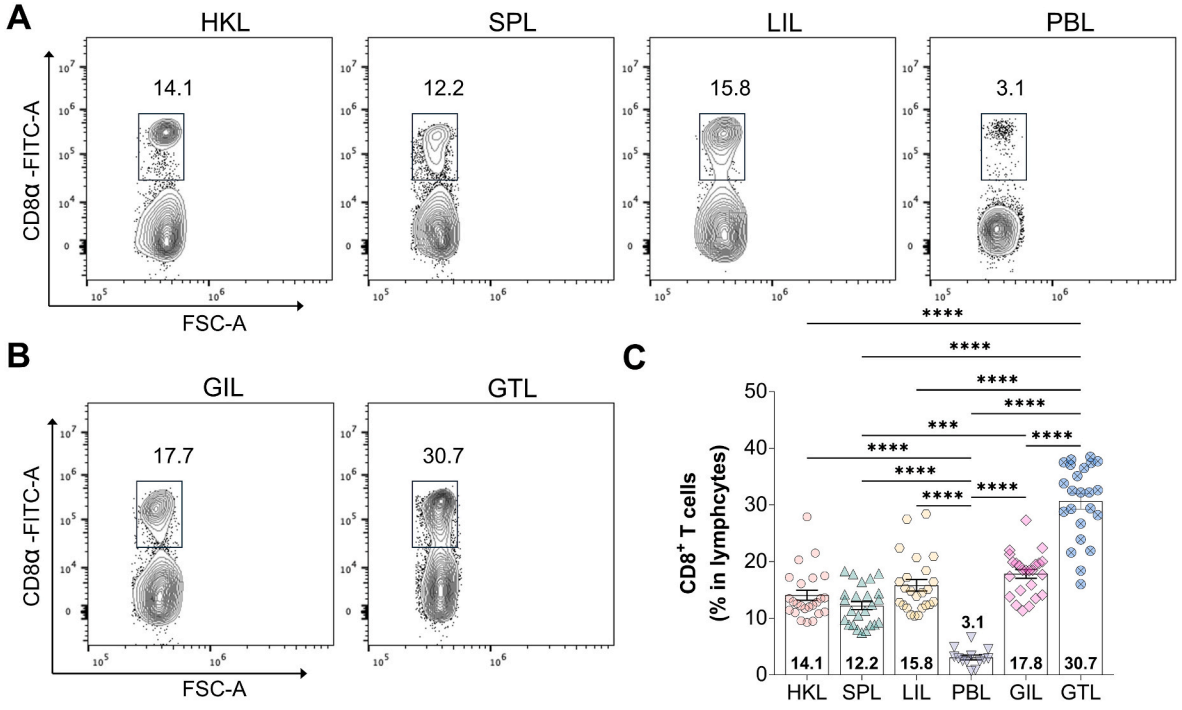

Fig. 4. Distribution of large yellow croaker $CD8^+$ T cell subsets in lymphoid tissues.
(A, B) Representative flow cytometry dot plots show croaker $CD8^+$ T cells within the lymphocyte population from head kidney (HKL), spleen (SPL), liver (LIL) and periphery blood (PBL) (A) and gills (GILs), gut (GTL) (B) stained with anti-CD8α mAb. The $CD8^+$ T cells are indicated in rectangle, the numbers adjacent to the rectangle show the percentage of $CD8^+$ T cells within the lymphocyte population of each tissue. (C) The mean percentage of $CD8^+$ T cells within the lymphocyte population of the indicated tissues beneath the columns. Data are representative of at least three independent experiments and expressed as means ± SEM. Each symbol represents an individual fish (n = 13–24 fish). Statistical analysis was performed by ordinary one-way ANOVA followed by Tukey's post hoc test. ***P < 0.001 and ****P < 0.0001. (For interpretation of the references to colour in this figure legend, the reader is referred to the Web version of this article.)

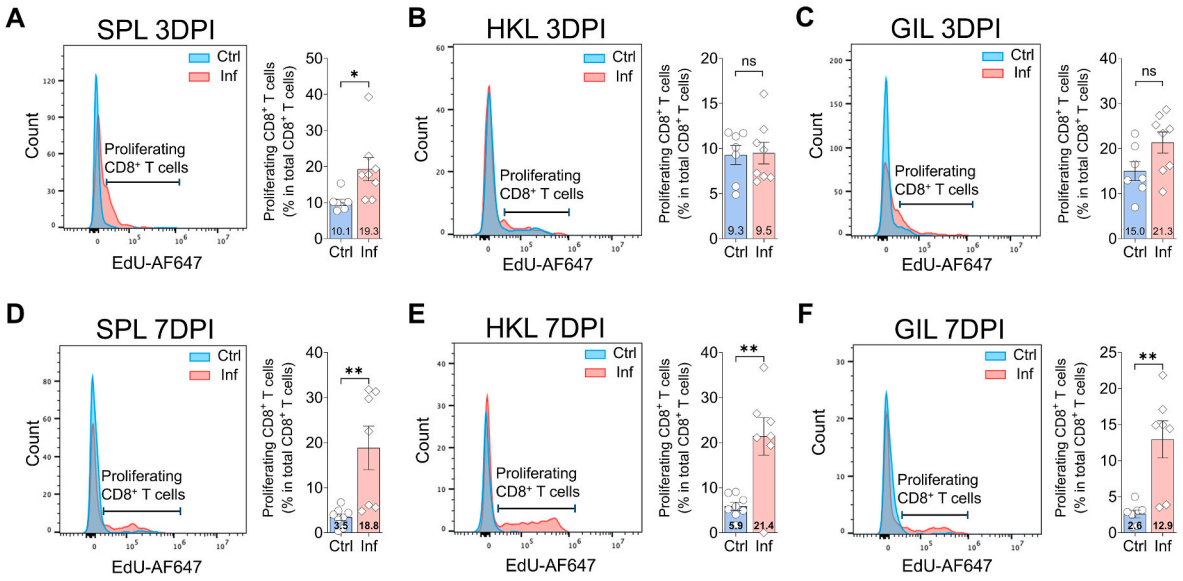

Fig. 5. Proliferating responses of CD8$^+$ T cells at 3 and 7 DPI upon Ci infection.
(A to C) Proliferation profiles of CD8$^+$ T cells in spleen (A), HK (B) and gills (C) tissues from control (Ctrl) and Ci-infected (Inf) fish after Ci infection at 3 DPI. (D to F) Proliferation profiles of CD8$^+$ T cells in spleen (D), HK (E) and gills (F) tissues from control and Ci-infected fish after Ci infection at 7 DPI. Representative overlaid histograms show the proliferating cells within CD8$^+$ T cell population from control (blue) and Ci-infected (orange) fish (left panels). Horizontal bracket lines indicate the proliferating population which are EdU positive. Bar plots present the percentage of proliferating cells within CD8$^+$ T cell population from control (blue) and Ci-infected (orange) fish (right panels). Data are representative of two independent experiments and presented as means ± SEM, each symbol represents an individual fish (n = 7–8 fish per group). Numbers within the bar plots indicate means. Statistical analysis was performed by two-tailed unpaired Student's t-test. *P < 0.05 and **P < 0.01. (For interpretation of the references to colour in this figure legend, the reader is referred to the Web version of this article.)

from infected fish were significantly higher compared to those from control fish (Fig. 6A and B), suggesting that CD8$^+$ T cells were activated and recruited to the focus of infection. The expression of *ifng* was upregulated upon Ci infection (Fig. 6C), supporting this observation, significantly higher levels of *granzyme a* (*gzma*), *gzmb*, and *perforin 1* (*prf1*) transcripts were also observed in gills CD8$^+$ T cells (Fig. 6D). Interestingly, *lymphocyte activation gene 3* (*lag3*), a T cell suppressor, showed an increased level of gene expression in the CD8$^+$ T cells in the infected fish (Fig. 6E), suggesting that CD8$^+$ T cell overactivation may be prevented to maintain their homeostasis.

3.7. Percentage of CD8$^+$ T cells declined in lymphocyte populations during the acute lethal infection

The proliferation and activation of CD8$^+$ T cells in the infected fish pointed to a persistent supply and replenishment of effector CD8$^+$ T cells, contributing to an expansion of this population to combat Ci invasion during the acute infection, a pattern commonly observed in mammals [37]. To this end, we assessed the proportions of proliferating and non-proliferating CD8$^+$ T cells to determine whether the CD8$^+$ T cell proliferation leads to an expansion upon Ci infection. To our surprise, minimal increase in proportion of CD8$^+$ T cells was observed in either proliferating or non-proliferating lymphocyte subsets across the indicated tissues (Fig. 7). In contrast, the proportion of CD8$^+$ T cells within the non-proliferating lymphocyte gate decreased in both the spleen and gills at 7 DPI. Specifically, the percentage of non-proliferating CD8$^+$ T cells declined from ~16.5 % in control fish to ~7.8 % in infected fish in the spleen, and from ~10.6 % to ~6.9 % in the gills (Fig. 7A and B, lower panels), suggesting that other lymphocytes predominated over resident CD8$^+$ T cells in those tissues during acute Ci infection.

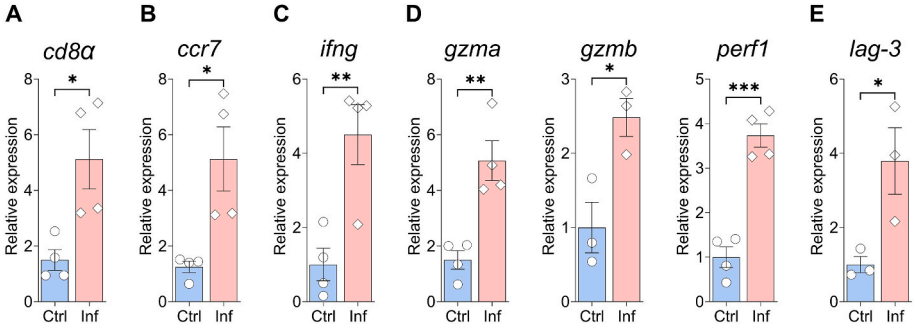

Fig. 6. Real-time PCR analysis of CTLs-associated genes in CD8$^+$ T cells from gills after Ci infection.
Relative transcript levels of *cd8α* (A), *ccr7* (B), *ifng*(C), *gzma*, *gzmb*, *perf1*(D) and *lag-3* (E) were assessed by qPCR in gills CD8$^+$ T cells from control and Ci-infected fish at 7 DPI. Expression levels in Ci-infected fish were normalized to those in control fish which were set as 1 (n = 3–4 fish per group). Data are representative of two independent experiments and expressed as mean ± SEM. Each symbol represents an individual fish. Statistical analysis was performed by two-tailed unpaired Student's t-test. *P < 0.05, **P < 0.01 and ***P < 0.001.

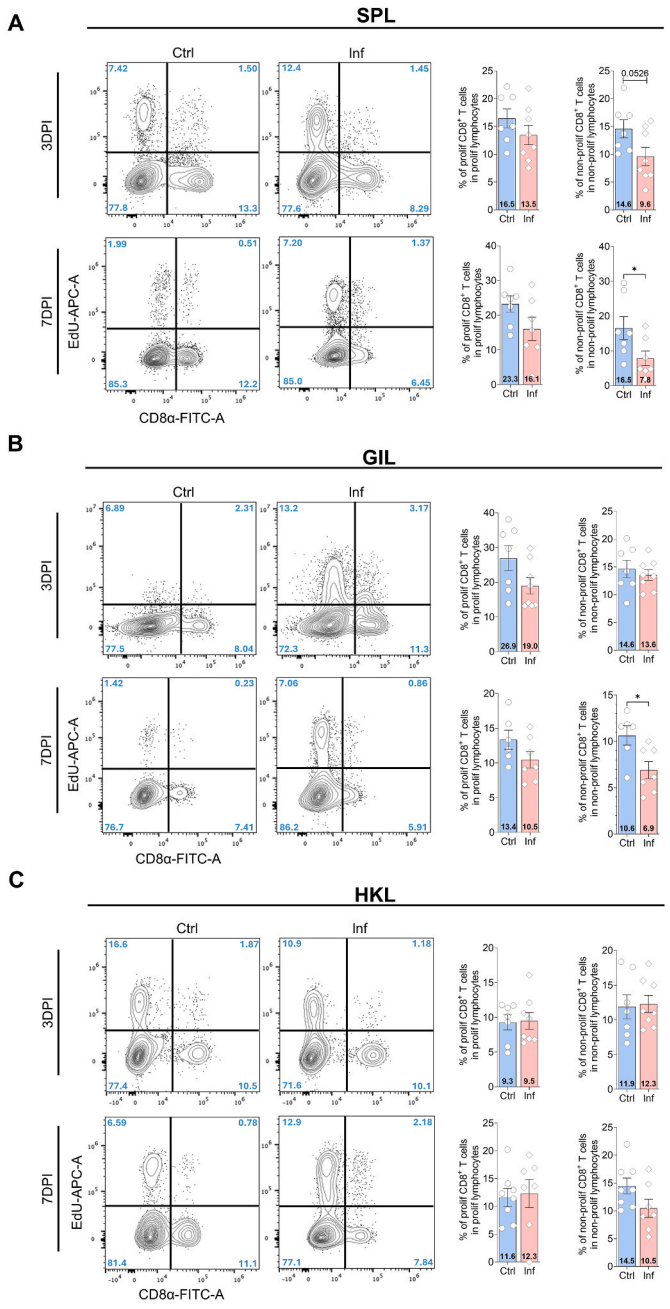

Fig. 7. Proportion of CD8$^+$ T cells within proliferating and non-proliferating lymphocyte populations upon Ci-infection.
Representative flow cytometry contour plots show that lymphocytes from spleen (A), gills (B) and HK (C) were gated for four subpopulations by co-staining with EdU and anti-CD8α, resulting in: proliferating CD8$^+$ T cells (EdU$^+$/CD8$^+$), proliferating CD8$^-$ lymphocytes (EdU$^+$/CD8$^-$), non-proliferating CD8$^+$ T cells (EdU$^-$/CD8$^+$) and non-proliferating CD8$^-$ lymphocytes (EdU$^-$/CD8$^-$). Numbers on contour plots present the percentage of each gated subpopulation. Bar plots present the percentages of proliferating CD8$^+$ T cells (EdU$^+$/CD8$^+$) in whole proliferating lymphocyte gates (EdU$^+$/CD8$^+$ plus EdU$^+$/CD8$^-$subpopulations), and non-proliferating CD8$^+$ T cells (EdU$^-$/CD8$^+$) in non-proliferating lymphocyte gates (Edu$^-$/CD8$^+$ plus Edu$^-$/CD8$^-$ subpopulations) from control and Ci-infected fish at 3 and 7 DPI. Data are representative of two independent experiments and expressed as mean ± SEM (n = 7–8 fish). Numbers within the bar plots indicate means. Each symbol represents an individual fish. Statistical analysis was performed by two-tailed unpaired Student's t-test. *$P < 0.05$, $P = 0.0526$ in the bar plot indicates a trend toward statistical significance.

3.8. Transient depletion of CD8$^+$ T cell occurred during the acute infection

To further understand whether the contraction of CD8$^+$ T cells in lymphocytes after infection was ascribed to the decrease in their abundance, we counted total lymphocyte and CD8$^+$ T cell numbers separately by flow cytometry under the same flow rate and normalized the counts to cells per second to compare the changes in CD8$^+$ T cells between control and infected fish. Our analysis revealed that a large depletion of CD8$^+$ T cells was observed in the HK and spleen during the acute infection from 3 to 7 DPI (Fig. 8A and B). Of particular note, compared with 551 and 1058 CD8$^+$ T cells counted in the HK and spleen of control fish, only 118 and 288 cells were detected in the corresponding tissues of infected fish, indicating that approximately 79 % of CD8$^+$ T cells in the HK and 73 % in the spleen were lost by day 7 post infection (Fig. 8B). In contrast, no significant changes in total lymphocytes were detected in infected fish compared to control fish (Fig. 8D). In the gills, both lymphocytes and CD8$^+$ T cells were significantly reduced to 57 % and 49 % of control levels, respectively, at day 3 post infection (Fig. 8A and C), followed by a rapid restoration to normal levels on day 7 (Fig. 8B and D). These data highlight that the local proliferation and migration from other immune tissues likely act to restore CD8$^+$ T cell homeostasis at the site of parasite infection, even though their depletion in systemic lymphoid tissues appeared unavoidable.

4. Discussion

CD8$^+$ T cells, which express the CD8 co-receptor, serve as loyal guardians of the immune system that remain ever ready to defend the host against invading pathogens [38]. As a critical arm of immune surveillance, CD8$^+$ T cells stand out among lymphocytes due to their primary function as cytotoxic killers that directly engage the infected cells or pathogens [38]. Over the past decades, fish lymphocytes have been extensively studied across various aquaculture species. However, most of these studies have predominantly focused on the IgM$^+$, IgT$^+$, CD4-1$^+$ and CD4-2$^+$ subsets, and their roles in adaptive immune responses against endogenous antigens or invading pathogens [39,40]. Despite the limited research on CD8$^+$ T cells in fish, a few studies have successfully overcome significant technical barriers to develop validated Abs for isolating and characterizing CD8$^+$ T cells [16,17,41]. In this study, we report the establishment of an anti-large yellow croaker CD8α mAb and provide a comprehensive analysis of the phenotypic and functional characteristics of croaker CD8$^+$ T cells. Notably, we demonstrate that dysregulation of croaker CD8$^+$ T cells during primary parasite infection closely resembles the recently described T cell exhaustion formed in acute infection [42], a phenomenon previously unrecognized in teleost species.

Using the newly developed anti-croaker CD8α mAbs, we sorted CD8$^+$ T cells and found that these cells exclusively expressed the transcripts of *cd8α* and *cd8β* genes, which are well-established markers defining CD8$^+$ T cells. In addition, expression of the T cell lineage marker *cd3e* was also detected in the sorted CD8$^+$ T cells. In contrast, transcripts of the fish B cell receptors (*ighm* and *ight*), and CD4 coreceptors (*cd4-1* and *cd4-2*) were only present in the CD8$^-$ lymphocytes, further validating that our mAb specifically and uniquely recognized croaker CD8$^+$ lymphocytes. Our findings are supported by morphological characteristics of CD8$^+$ T cells previously described in both fish species and mammals [43,44].

A remarkable disparity in the distribution of croaker CD8$^+$ T cells was observed across various tissues in our study. Notably, CD8$^+$ T cells were more abundant in MALTs compared to secondary lymphoid organs, but were relatively low in the circulation. Their preference for residing in MALTs aligns with the pattern found in humans, mice, and other teleost fish [45,46], underscoring the key role of CD8$^+$ T cells in frontline defense at mucosal surfaces continuously exposed to microbial and dietary antigens [47]. However, the abundance of CD8$^+$ T cells in the HK and spleen remains controversial across fish species. For

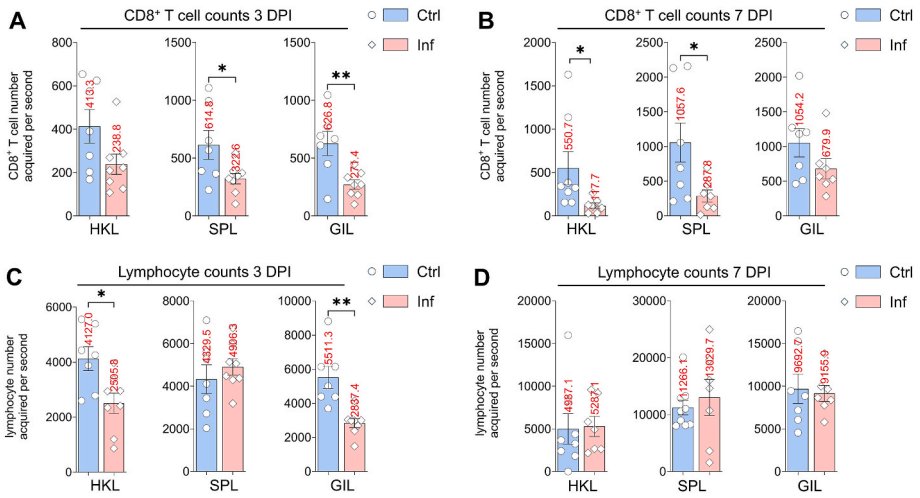

Fig. 8. Reduction of total CD8$^+$ T cells in numbers during the acute Ci infection. Lymphocytes were isolated from each organ or tissue in equal amounts and processed in parallel with the same volume of cell culture medium and staining solutions. The stained cells were eventually resuspended in an equal volume of loading solution and acquired at a consistent flow rate by flow cytometry. All cell counts obtained by flow cytometry were normalized to events per second to ensure an accurate comparison of cell numbers. (A and B) Number of CD8$^+$ T cells from HK, spleen and gills at 3 days (A) and 7 days (B) post Ci infection. (C and D) Number of lymphocytes from HK, spleen and gills at 3 days (C) and 7 days (D) post Ci infection. Data are representative of two independent experiments and expressed as mean ± SEM (n = 7–8 fish). Vertical numbers above the bar plots indicate means. Each symbol represents an individual fish. Statistical analysis was performed by two-tailed unpaired Student's t-test. *$P < 0.05$ and **$P < 0.01$.

instance, they accounted for ~3 % SPL and HKL in flounder, whereas ~7.7 %–~8.7 % in sea bass [17,44]. The differences in CD8$^+$ T cell abundance across species can be attributed to the species diversity, environmental factors, microbiota composition, age-related immune variations and evolutionary differences in immune system architecture [24,48,49]. Regardless, we found that croaker CD8$^+$ T cells constituted the highest proportions in those two secondary lymphoid organs compared to other fish species so far. Interestingly, croaker liver contained a substantial population of CD8$^+$ T cells even slightly higher than the spleen and HK. Although the liver is not considered a classic secondary lymphoid organ in humans, it is often regarded as a systemic lymphoid tissue to a certain extent due to a large accumulation of immune cells that are actively involved in immunosurveillance. In particular, the liver is well-positioned to encounter and process the antigens that continuously enter from the gut [50,51]. The liver-resident CD8$^+$ T cells in humans were uniquely adapted to the hepatic microenvironment, where they predominantly differentiated into tissue-resident memory cells. These findings provide us with new insights into the tissue-associated heterogeneity of croaker CD8$^+$ T cells.

Once primed by antigenic or pathogenic stimulation, quiescent CD8$^+$ T cells undergo rapid proliferation and differentiation into cytotoxic effectors that release granules containing perforin and granzymes to eliminate pathogens [52,53]. To date, the cytotoxic activities of fish CTLs have been primarily investigated in ginbuna crucian carp, in which CD8$^+$ T cells have been shown to kill allogeneic cells [54], virus-infected cells [55] and eliminate intracellular bacteria in internal organs [56]. More interestingly, CD8$^+$ T cells derived from the HK and gills of ginbuna carp exerted cytotoxicity against extracellular protozoan parasites, a process mediated by serine proteases and perforin [22]. This represents the first evidence that fish CTLs can eliminate parasites in a contact-dependent manner [22]. The study in orange spotted grouper further demonstrated that the cytotoxic activity against Ci was enhanced after immunization with parasite-derived heat shock protein 70C [23]. However, the activation and differentiation dynamics of fish CD8$^+$ T cells following pathogen infection remain poorly understood. In species such as sea bass and flounder, increased proportions of CD8$^+$ T cells or elevated *cd8* transcript levels have been observed in the HK, spleen, MALTs, and even in non-lymphoid tissues from the KLH-immunized fish [11,17,57]. However, changes in percentages or transcripts were less informative than direct proliferation analysis for determining whether these variations arose from shifts in lymphocyte composition or from increased *cd8* gene expression within the same population of cells. To this end, we infected large yellow croaker with the most common marine parasite, Ci, and observed a strong systemic proliferation of croaker CD8$^+$ T cells occurring in the HK and spleen of infected fish, suggesting a possibility that the captured parasite antigens were transported to systemic lymphoid organs, where effector CTLs were activated and differentiated as reported in mammals [58].

A profound increase in EdU$^+$ CD8$^+$ T cells in the gills of infected fish suggests a local proliferative response of CD8$^+$ T cells at the site of parasite infection. However, the possibility that proliferating CD8$^+$ T cells migrated from other lymphoid organs cannot be ruled out, given the increased expression of chemokine receptor *ccr7* in gill CD8$^+$ T cells. The local proliferation of CD8$^+$ T cells in gills took place simultaneously with the upregulation of *cd8α* transcripts in the sorted gills CD8$^+$ T cells after infection. Moreover, croaker CD8$^+$ T cells were activated after parasite infection and differentiated into the on-site effector CTLs, as indicated by the significant induction of *grzma*, *grzmb*, *prf1* and *ifng* in gill CD8$^+$ T cells, which are hallmark genes of activated CTLs involved in target elimination [59]. Similarly, these CTL effector genes have been found strongly up-regulated in trout CD8α + lymphocytes upon a mitogen, PHA stimulation [16]. The transfer of CD8$^+$ T cells from donor carps previously exposed to bacterial pathogen markedly induced the expression of *prf* and *ifng* genes in HKL and SPL of recipients [60]. Collectively, our study, together with previous studies, has documented a universal principle of effector CTLs that has arisen in the ancient vertebrates prior to the emergence of tetrapods.

Under typical circumstances, CD8$^+$ T cells undergo a large-scale expansion in response to viruses, bacteria, and parasites, driven by robust proliferation triggered by pathogenic antigens during acute infections. Contrary to expectations, our results revealed a remarkable depletion of CD8$^+$ T cells in the gills 3 days (early phase) post parasite infection, which was followed by a recovery to near-normal levels at day 7 (late phase). The restoration of gill CD8$^+$ T cells during the late phase of infection appeared to be compensated by the migration of cells from the HK and spleen, where CD8$^+$ T cell numbers had declined by more than 70 % compared to control fish. This pronounced reduction may be attributed to apoptosis, a phenomenon previously observed in tilapia following challenge with *Edwardsiella piscicida* [8]. The potential contribution of CD8$^+$ T cell apoptosis to this depletion during acute

infection warrants further investigation. Other potential mechanisms may also contribute to this loss. For example, $CD8^+$ T cells may have migrated from systemic lymphoid organs to peripheral infection sites such as the skin. However, our study focused primarily on gills dynamics, and the skin compartment was not examined. In gilthead sea bream infected with the intestinal parasite *Enteromyxum leei*, the expression of *cd8α* and *cd8β* were down-regulated in the HK, but up-regulated in the anterior intestine [61], further supporting the possibility of tissue-specific migration which cannot be ruled out in our study. Additionally, the acute and lethal nature of the infection may induce T cell exhaustion as reported in human [42], leading to functional impairment and reduced cell numbers. However, our study did not include functional assays or supporting metadata to directly assess T cell exhaustion, representing another limitation that should be addressed in future investigations. Interestingly, the proliferation of $CD8^+$ T cells in the HK and spleen was insufficient to replenish the consumed population, thus leading to a persistent depletion of $CD8^+$ T cells during the acute phase of infection. Our results can be supported by the notion that lymphopenia can be caused by several fatal viruses, such as SARS-CoV-2, Ebola virus (EBOV), and human immunodeficiency virus (HIV), particularly in severely or critically ill individuals who exhibit significantly lower lymphocyte counts compared to healthy, mildly ill, or recovered patients. This phenomenon highlighted a close association between the degree of lymphocyte counts and disease severity [62–64]. In a similar vein, a significant reduction of $CD8^+$ T cells was found in large yellow croaker suffering from a severe Ci infection, which resulted in mortality exceeding 80 % in our facility. Moreover, the fact that the total lymphocyte counts remained unchanged in the late phase of acute infection suggests an expansion of other lymphocyte types to replace the decreased $CD8^+$ T cells. However, this expansion was insufficient to protect fish from a lethal dose of Ci infection, underscoring that the acute infection caused by Ci is strongly associated with $CD8^+$ T cell depletion.

5. Conclusion

In conclusion, we developed a novel mAb targeting the CD8α of large yellow croaker and characterized the fundamental features of croaker $CD8^+$ T cells. The robust proliferation of $CD8^+$ T cell and their active expression of cytotoxic factors in response to Ci highlight the critical role of croaker CTLs in host defense and parasite clearance. These findings suggest that $CD8^+$ T cells potentially serve both as valuable biomarkers for monitoring fish health and tools for disease surveillance in aquaculture. In particular, our study provides the first evidence of $CD8^+$ T cell depletion under severe parasitic infection in a teleost species, thus offering critical insights into the design of vaccines that aim to induce protective $CD8^+$ T cell responses to prevent such infections. Such strategies may help reduce the substantial losses in fish production caused by parasitic diseases in aquaculture.

CRediT authorship contribution statement

Guolong Lai: Writing – review & editing, Writing – original draft, Investigation, Formal analysis, Visualization, Data curation, Validation. **Xinran Li:** Methodology, Investigation, Data curation, Validation. **Sichang Liu:** Investigation, Data curation. **Luyang Zhao:** Investigation, Data curation. **Mengtian Xie:** Investigation, Data curation. **Li Huang:** Data curation. **Wenxuan Zhang:** Data curation. **Wenbing Bao:** Data curation. **Yan Lin:** Methodology. **Yang Ding:** Writing – review & editing, Writing – original draft, Supervision, Project administration, Methodology, Conceptualization, Validation, Visualization, Funding acquisition. **Xinhua Chen:** Writing – review & editing, Writing – original draft, Supervision, Resources, Project administration, Methodology, Conceptualization, Funding acquisition.

Funding

This research was supported by the National Natural Science Foundation of China (U23A20253, 31802337), International Postdoctoral Exchange Fellowship Program by the Office of China Postdoctoral Council (PC2018016), and China Agriculture Research System of MOF and MARA (CARS-47).

Declaration of competing interest

Authors declare no competing interests.

Acknowledgements

We would like to thank Prof. Hui Gong from the Institute of Biotechnology (FAAS, Fuzhou, China), for kindly providing valuable suggestions. Our gratitude also extends to Dr. Xin-Zhan Meng and Dr. Yingyi Duan from Xiamen University for their insightful feedback and constructive discussions.

Appendix A. Supplementary data

Supplementary data to this article can be found online at https://doi.org/10.1016/j.fsi.2025.110596.

Data availability

No data was used for the research described in the article.

References

[1] M.D. Cooper, M.N. Alder, The evolution of adaptive immune systems, Cell 124 (4) (2006) 815–822.
[2] M.H. Andersen, D. Schrama, P. Thor Straten, J.C. Becker, Cytotoxic T cells, J. Invest. Dermatol. 126 (1) (2006) 32–41.
[3] D.K. Cole, G.F. Gao, CD8: adhesion molecule, co-receptor and immuno-modulator, Cell. Mol. Immunol. 1 (2) (2004) 81–88.
[4] T. Yamaguchi, F. Takizawa, M. Furihata, V. Soto-Lampe, J.M. Dijkstra, U. Fischer, Teleost cytotoxic T cells, Fish Shellfish Immunol. 95 (2019) 422–439.
[5] J. Rossjohn, S. Gras, J.J. Miles, S.J. Turner, D.I. Godfrey, J. McCluskey, T cell antigen receptor recognition of antigen-presenting molecules, Annu. Rev. Immunol. 33 (2015) 169–200.
[6] A.K. Sewell, U.C. Gerth, D.A. Price, M.A. Purbhoo, J.M. Boulter, G.F. Gao, J.I. Bell, R.E. Phillips, B.K. Jakobsen, Antagonism of cytotoxic T-lymphocyte activation by soluble CD8, Nat. Med. 5 (4) (1999) 399–404.
[7] J.D. Hansen, P. Strassburger, Description of an ectothermic TCR coreceptor, CD8 alpha, in rainbow trout, J. Immunol. 164 (6) (2000) 3132–3139.
[8] H. Suetake, K. Araki, K. Akatsu, T. Somamoto, J.M. Dijkstra, Y. Yoshiura, K. Kikuchi, Y. Suzuki, Genomic organization and expression of CD8alpha and CD8beta genes in fugu *Takifugu rubripes*, Fish Shellfish Immunol. 23 (5) (2007) 1107–1118.
[9] T. Somamoto, Y. Yoshiura, T. Nakanishi, M. Ototake, Molecular cloning and characterization of two types of CD8alpha from ginbuna crucian carp, *Carassius auratus langsdorfii*, Dev. Comp. Immunol. 29 (8) (2005) 693–702.
[10] Z. Guo, G.L. Wang, J.P. Fu, P. Nie, Characterization and expression of Cd8 molecules in Mandarin fish *Siniperca chuatsi*, J. Fish. Biol. 82 (1) (2013) 189–205.
[11] G. Kato, K. Goto, I. Akune, S. Aoka, H. Kondo, I. Hirono, CD4 and CD8 homologues in Japanese flounder, *Paralichthys olivaceus*: differences in the expressions and localizations of CD4-1, CD4-2, CD8α and CD8β, Dev. Comp. Immunol. 39 (3) (2013) 293–301.
[12] U. Fischer, K. Utke, M. Ototake, J.M. Dijkstra, B. Köllner, Adaptive cell-mediated cytotoxicity against allogeneic targets by CD8-positive lymphocytes of rainbow trout (*Oncorhynchus mykiss*), Dev. Comp. Immunol. 27 (4) (2003) 323–337.
[13] H. Toda, Y. Shibasaki, T. Koike, M. Ohtani, F. Takizawa, M. Ototake, T. Moritomo, T. Nakanishi, Alloantigen-specific killing is mediated by CD8-positive T cells in fish, Dev. Comp. Immunol. 33 (4) (2009) 646–652.
[14] K. Li, Y. Zhu, Z. Fang, M. Geng, J. Zhang, Y. Zheng, Y. Cao, X. Wei, J. Yang, Fish requires FasL to facilitate $CD8^+$ T-cell function and antimicrobial immunity, J. Immunol. (2025).
[15] X. Wu, J. Xing, X. Tang, X. Sheng, H. Chi, W. Zhan, Protective cellular and humoral immune responses to Edwardsiella tarda in flounder (*Paralichthys olivaceus*) immunized by an inactivated vaccine, Mol. Immunol. 149 (2022) 77–86.
[16] F. Takizawa, J.M. Dijkstra, P. Kotterba, T. Korytář, H. Kock, B. Köllner, B. Jaureguiberry, T. Nakanishi, U. Fischer, The expression of CD8α discriminates distinct T cell subsets in teleost fish, Dev. Comp. Immunol. 35 (7) (2011) 752–763.
[17] X. Jiang, J. Xing, X. Tang, X. Sheng, H. Chi, W. Zhan, CD4-1 and CD8α T lymphocytes subsets in spotted sea bass (*Lateolabrax maculatus*) and comparison on

antigenicity of T lymphocytes subsets in other three marine fish species, Fish Shellfish Immunol. 131 (2022) 487–497.
[18] A.S. Dalum, L. Austbø, H. Bjørgen, K. Skjødt, I. Hordvik, T. Hansen, P.G. Fjelldal, C. M. Press, D.J. Griffiths, E.O. Koppang, The interbranchial lymphoid tissue of Atlantic Salmon (*Salmo salar L*) extends as a diffuse mucosal lymphoid tissue throughout the trailing edge of the gill filament, J. Morphol. 276 (9) (2015) 1075–1088.
[19] R. Castro, F. Takizawa, W. Chaara, A. Lunazzi, T.H. Dang, B. Koellner, E. Quillet, A. Six, U. Fischer, P. Boudinot, Contrasted TCRβ diversity of $CD8^+$ and $CD8^-$ T cells in rainbow trout, PLoS One 8 (4) (2013) e60175.
[20] A.G. Granja, E. Leal, J. Pignatelli, R. Castro, B. Abós, G. Kato, U. Fischer, C. Tafalla, Identification of teleost skin $CD8\alpha^+$ dendritic-like cells, representing a potential common ancestor for mammalian cross-presenting dendritic cells, J. Immunol. 195 (4) (2015) 1825–1837.
[21] D.L. Hetland, O.B. Dale, K. Skjødt, C.M. Press, K. Falk, Depletion of CD8 alpha cells from tissues of Atlantic salmon during the early stages of infection with high or low virulent strains of infectious salmon anaemia virus (ISAV), Dev. Comp. Immunol. 35 (8) (2011) 817–826.
[22] M. Sukeda, K. Shiota, M. Kondo, T. Nagasawa, M. Nakao, T. Somamoto, Innate cell-mediated cytotoxicity of $CD8(^+)$ T cells against the protozoan parasite *Ichthyophthirius multifiliis* in the ginbuna crucian carp, *Carassius auratus langsdorfii*, Dev. Comp. Immunol. 115 (2021) 103886.
[23] T. Josepriya, K.-H. Chien, H.-Y. Lin, H.-N. Huang, C.-J. Wu, Y.-L. Song, Immobilization antigen vaccine adjuvanted by parasitic heat shock protein 70C confers high protection in fish against *cryptocaryonosis*, Fish Shellfish Immunol. 45 (2) (2015) 517–527.
[24] M. Terekhova, A. Swain, P. Bohacova, E. Aladyeva, L. Arthur, A. Laha, D. A. Mogilenko, S. Burdess, V. Sukhov, D. Kleverov, B. Echalar, P. Tsurinov, R. Chernyatchik, K. Husarcikova, M.N. Artyomov, Single-cell atlas of healthy human blood unveils age-related loss of $NKG2C(^+)GZMB(-)CD8(^+)$ memory T cells and accumulation of type 2 memory T cells, Immunity 56 (12) (2023) 2836–2854. e9.
[25] Y. Li, B. Jiang, Z. Mo, A. Li, X. Dan, Cryptocaryon irritans (Brown, 1951) is a serious threat to aquaculture of marine fish, Rev. Aquacult. 14 (1) (2022) 218–236.
[26] L. Zhou, R. Zhou, X. Xie, F. Yin, Characteristics and risk assessment of cryptocaryoniasis in large yellow croaker (*Larimichthys crocea*) at different densities in industrialized aquaculture, Aquaculture 582 (2024) 740501.
[27] J. Ao, Y. Mu, L.X. Xiang, D. Fan, M. Feng, S. Zhang, Q. Shi, L.Y. Zhu, T. Li, Y. Ding, L. Nie, Q. Li, W.R. Dong, L. Jiang, B. Sun, X. Zhang, M. Li, H.Q. Zhang, S. Xie, Y. Zhu, X. Jiang, X. Wang, P. Mu, W. Chen, Z. Yue, Z. Wang, J. Wang, J.Z. Shao, X. Chen, Genome sequencing of the perciform fish *Larimichthys crocea* provides insights into molecular and genetic mechanisms of stress adaptation, PLoS Genet. 11 (4) (2015) e1005118.
[28] Y. Ding, J. Ao, C. Ai, X. Chen, Molecular and functional identification of three interleukin-17A/F (IL-17A/F) homologues in large yellow croaker (*Larimichthys crocea*), Dev. Comp. Immunol. 55 (2016) 221–232.
[29] Z. Cui, H. Zhao, X. Chen, Molecular and functional characterization of two IgM subclasses in large yellow croaker (*Larimichthys crocea*), Fish Shellfish Immunol. 134 (2023) 108581.
[30] Y. Ding, Y. Zhang, Y. Shen, Y. Zhang, Z. Li, Y. Shi, Z. Cui, X. Chen, Aggregation and proliferation of B cells and T cells in MALTs upon *Cryptocaryon irritans* infection in large yellow croaker *Larimichthys crocea*, Fish Shellfish Immunol. 149 (2024) 109535.
[31] P. Mu, J. Huo, X. Li, W. Li, X. Li, J. Ao, X. Chen, IL-2 signaling couples the MAPK and mTORC1 axes to promote T cell proliferation and differentiation in teleosts, J. Immunol. 208 (7) (2022) 1616–1631.
[32] F. Takizawa, S. Magadan, D. Parra, Z. Xu, T. Korytář, P. Boudinot, J.O. Sunyer, Novel teleost CD4-bearing cell populations provide insights into the evolutionary origins and primordial roles of $CD4^+$ lymphocytes and $CD4^+$ macrophages, J. Immunol. 196 (11) (2016) 4522–4535.
[33] Y. Huang, X. Yuan, P. Mu, Q. Li, J. Ao, X. Chen, Development of monoclonal antibody against IgM of large yellow croaker (*Larimichthys crocea*) and characterization of IgM^+ B cells, Fish Shellfish Immunol. 91 (2019) 216–222.
[34] E.J.W. Geven, P.H.M. Klaren, The teleost head kidney: integrating thyroid and immune signalling, Dev. Comp. Immunol. 66 (2017) 73–83.
[35] Z. Mo, H. Wu, Y. Hu, X. Lai, W. Guo, Y. Duan, X. Dan, Y. Li, Protection of grouper against *Cryptocaryon irritans* by immunization with Tetrahymena thermophila and protective cross-reactive antigen identification, Front. Immunol. 13 (2022) 891643.
[36] K. Yang, A. Kallies, Tissue-specific differentiation of CD8(+) resident memory T cells, Trends Immunol. 42 (10) (2021) 876–890.
[37] R.J. Johnston, L. Comps-Agrar, J. Hackney, X. Yu, M. Huseni, Y. Yang, S. Park, V. Javinal, H. Chiu, B. Irving, D.L. Eaton, J.L. Grogan, The immunoreceptor TIGIT regulates antitumor and antiviral CD8(+) T cell effector function, Cancer Cell 26 (6) (2014) 923–937.
[38] P. Wong, E.G. Pamer, CD8 T cell responses to infectious pathogens, Annu. Rev. Immunol. 21 (2003) 29–70, 21, 2003.
[39] I. Salinas, Á. Fernández-Montero, Y. Ding, J.O. Sunyer, Mucosal immunoglobulins of teleost fish: a decade of advances, Dev. Comp. Immunol. 121 (2021) 104079.
[40] I. Salinas, Y. Ding, Á. Fernández-Montero, J.O. Sunyer, Mucosal Immunity in Fish, Principles of Fish Immunology: from Cells and Molecules to Host Protection, Springer, 2022, pp. 387–443.
[41] R. Miyazawa, Y. Matsuura, Y. Shibasaki, S. Imamura, T. Nakanishi, Cross-reactivity of monoclonal antibodies against CD4-1 and CD8α of ginbuna crucian carp with lymphocytes of zebrafish and other cyprinid species, Dev. Comp. Immunol. 80 (2018) 15–23.
[42] T. Chu, M. Wu, B. Hoellbacher, G.P. de Almeida, C. Wurmser, J. Berner, L. V. Donhauser, A.-K. Gerullis, S. Lin, J.D. Cepeda-Mayorga, I.I. Kilb, L. Bongers, F. Toppeta, P. Strobl, B. Youngblood, A.M. Schulz, A. Zippelius, P.A. Knolle, M. Heinig, C.-P. Hackstein, D. Zehn, Precursors of exhausted T cells are pre-emptively formed in acute infection, Nature (2025).
[43] M. Sung, J.H. Kim, H.S. Min, S. Jang, J. Hong, B.K. Choi, J. Shin, K.S. Chung, Y. R. Park, Three-dimensional label-free morphology of $CD8^+$ T cells as a sepsis biomarker, Light Sci. Appl. 12 (1) (2023) 265.
[44] J. Xing, J. Ma, X. Tang, X. Sheng, W. Zhan, Characterizations of CD4-1, CD4-2 and CD8β T cell subpopulations in peripheral blood leucocytes, spleen and head kidney of Japanese flounder (*Paralichthys olivaceus*), Mol. Immunol. 85 (2017) 155–165.
[45] S. Chandra, G. Ascui, T. Riffelmacher, A. Chawla, C. Ramírez-Suástegui, V. C. Castelan, G. Seumois, H. Simon, M.P. Murray, G.Y. Seo, A.L.R. Premlal, B. Schmiedel, G. Verstichel, Y. Li, C.H. Lin, J. Greenbaum, J. Lamberti, R. Murthy, J. Nigro, H. Cheroutre, C.H. Ottensmeier, S.M. Hedrick, L.F. Lu, P. Vijayanand, M. Kronenberg, Transcriptomes and metabolism define mouse and human MAIT cell populations, Sci. Immunol. 8 (89) (2023) eabn8531.
[46] J.H. Rombout, L. Abelli, S. Picchietti, G. Scapigliati, V. Kiron, Teleost intestinal immunology, Fish Shellfish Immunol. 31 (5) (2011) 616–626.
[47] R.S. Thwaites, A.S.S. Uruchurtu, V.A. Negri, M.E. Cole, N. Singh, N. Poshai, D. Jackson, K. Hoschler, T. Baker, I.C. Scott, X.R. Ros, E.S. Cohen, M. Zambon, K. M. Pollock, T.T. Hansel, P.J.M. Openshaw, Early mucosal events promote distinct mucosal and systemic antibody responses to live attenuated influenza vaccine, Nat. Commun. 14 (1) (2023) 8053.
[48] J. Cong, P. Liu, Z. Han, W. Ying, C. Li, Y. Yang, S. Wang, J. Yang, F. Cao, J. Shen, Y. Zeng, Y. Bai, C. Zhou, L. Ye, R. Zhou, C. Guo, C. Cang, D.L. Kasper, X. Song, L. Dai, L. Sun, W. Pan, S. Zhu, Bile acids modified by the intestinal microbiota promote colorectal cancer growth by suppressing CD8(+) T cell effector functions, Immunity 57 (4) (2024) 876–889.e11.
[49] T. Masubuchi, L. Chen, N. Marcel, G.A. Wen, C. Caron, J. Zhang, Y. Zhao, G. P. Morris, X. Chen, S.M. Hedrick, L.F. Lu, C. Wu, Z. Zou, J.D. Bui, E. Hui, Functional differences between rodent and human PD-1 linked to evolutionary divergence, Sci. Immunol. 10 (103) (2025) eads6295.
[50] K. Kawashima, F. Andreata, C.G. Beccaria, M. Iannacone, Priming and maintenance of adaptive immunity in the liver, Annu. Rev. Immunol. 42 (1) (2024) 375–399.
[51] R. Castro, B. Abós, J. Pignatelli, L. von Gersdorff Jørgensen, A. González Granja, K. Buchmann, C. Tafalla, Early immune responses in rainbow trout liver upon viral hemorrhagic septicemia virus (VHSV) infection, PLoS One 9 (10) (2014) e111084.
[52] J. Xu, N. Yang, T. Xie, G. Yang, L. Chang, D. Yan, T. Li, Summary and comparison of the perforin in teleosts and mammals: a review, Scand. J. Immunol. 94 (1) (2021) e13047.
[53] Y. Cao, J. Zhang, D. Wang, Y. Zheng, J. Cheng, M. Geng, K. Li, J. Yang, X. Wei, Granzyme B secreted by T cells is involved in anti-bacterial immune response of tilapia, Fish Shellfish Immunol. 153 (2024) 109865.
[54] T. Somamoto, N. Okamoto, T. Nakanishi, M. Ototake, M. Nakao, In vitro generation of viral-antigen dependent cytotoxic T-cells from ginbuna crucian carp, *Carassius auratus langsdorfii*, Virology 389 (1–2) (2009) 26–33.
[55] S. Tajimi, M. Kondo, T. Nakanishi, T. Nagasawa, M. Nakao, T. Somamoto, Generation of virus-specific $CD8(^+)$ T cells by vaccination with inactivated virus in the intestine of ginbuna crucian carp, Dev. Comp. Immunol. 93 (2019) 37–44.
[56] S.K. Nayak, Y. Shibasaki, T. Nakanishi, Immune responses to live and inactivated Nocardia seriolae and protective effect of recombinant interferon gamma (rIFN γ) against nocardiosis in ginbuna crucian carp, *Carassius auratus langsdorfii*, Fish Shellfish Immunol. 39 (2) (2014) 354–364.
[57] J. Xing, K. Luo, Y.e. Xiao, X. Tang, W. Zhan, Influence of CD4-1^+, CD4-2^+ and CD8 $^+$ T lymphocytes subpopulations on the immune response of B lymphocytes in flounder (*Paralichthys olivaceus*) immunized with thymus-dependent or thymus-independent antigen, Fish Shellfish Immunol. 84 (2019) 979–986.
[58] B.J. Manfras, S. Reuter, T. Wendland, P. Kern, Increased activation and oligoclonality of peripheral $CD8(^+)$ T cells in the chronic human helminth infection alveolar echinococcosis, Infect. Immun. 70 (3) (2002) 1168–1174.
[59] I. Voskoboinik, J.C. Whisstock, J.A. Trapani, Perforin and granzymes: function, dysfunction and human pathology, Nat. Rev. Immunol. 15 (6) (2015) 388–400.
[60] M. Yamasaki, K. Araki, T. Nakanishi, C. Nakayasu, A. Yamamoto, Role of $CD4^+$ and $CD8\alpha^+$ T cells in protective immunity against Edwardsiella tarda infection of ginbuna crucian carp, Carassius auratus langsdorfii, Fish Shellfish Immunol. 36 (1) (2014) 299–304.
[61] M.C. Piazzon, I. Estensoro, J.A. Calduch-Giner, R. Del Pozo, A. Picard-Sánchez, J. Pérez-Sánchez, A. Sitjà-Bobadilla, Hints on T cell responses in a fish-parasite model: *Enteromyxum leei* induces differential expression of T cell signature molecules depending on the organ and the infection status, Parasit vectors 11 (2018) 1–17.
[62] Q. Ruan, K. Yang, W. Wang, L. Jiang, J. Song, Clinical predictors of mortality due to COVID-19 based on an analysis of data of 150 patients from Wuhan, China, Intensive Care Med. 46 (5) (2020) 846–848.
[63] R.M. Mingo, J.A. Simmons, C.J. Shoemaker, E.A. Nelson, K.L. Schornberg, R. S. D'Souza, J.E. Casanova, J.M. White, Ebola virus and severe acute respiratory syndrome coronavirus display late cell entry kinetics: evidence that transport to $NPC1^+$ endolysosomes is a rate-defining step, J. Virol. 89 (5) (2015) 2931–2943.
[64] S. Rajsic, R. Breitkopf, D. Kojic, Z. Bukumiric, B. Treml, Extracorporeal life support for patients with newly diagnosed HIV and acute respiratory distress syndrome: a systematic review and analysis of individual patient data, Asaio J. 69 (12) (2023) e513–e519.